

## Phase Behavior of the Au(111) Surface: Discommensurations and Kinks

K. G. Huang and Doon Gibbs

*Department of Physics, Brookhaven National Laboratory, Upton, New York 11973-5000*

D. M. Zehner

*Solid State Division, Oak Ridge National Laboratory, Oak Ridge, Tennessee 37831-6057*

A. R. Sandy and S. G. J. Mochrie

*Department of Physics, Massachusetts Institute of Technology, Cambridge, Massachusetts 02139-4307*

(Received 27 July 1990)

The clean Au(111) surface is found, using x-ray diffraction, to reconstruct between 300 and 1250 K with two distinct phases. Below 865 K, the surface structure consists of an equilibrium density of kinks between rotationally equivalent domains, each of which is itself composed of a sequence of uniaxial discommensurations. Above 880 K, the arrangement of kinks and discommensurations is disordered, which results in an isotropic compression of the reconstructed layer. The phase transition between the two structures is first order.

PACS numbers: 68.35.Rh, 61.10.Lx, 64.70.Kb

Studies of the thermal behavior of clean metal surfaces provide important information for understanding the atomic mechanisms that underlie surface reconstruction. Perhaps the most unusual reconstruction of a metal surface is that of the close-packed (111) face of gold. This surface has been studied extensively at 300 K by many techniques.<sup>1-10</sup> As a result, it is believed that the reconstruction may be described as a sequence of uniaxial discommensurations, separating surface regions with *ABC* stacking from regions with faulted *ABA* stacking [ $(p \times \sqrt{3})$  reconstruction, with  $p=23$ ]. Little is known, however, about the structural behavior at elevated temperatures. For this reason, we have carried out a comprehensive x-ray-diffraction study of the clean Au(111) surface between 300 and 1250 K. Our results have relevance to the suggestion that the relief of surface stress gives rise to the Au(111) reconstruction,<sup>11</sup> and to calculations which predict that high-symmetry surfaces, which may reconstruct into one of several rotationally equivalent structures, are unstable to the formation of domains.<sup>12</sup>

We have identified and characterized two distinct phases of the Au(111) surface. For  $T < 865$  K, the x-ray-diffraction pattern cannot be explained solely on the basis of the  $(p \times \sqrt{3})$  reconstruction. Instead, its interpretation leads to a structural model involving an equilibrium density of kinks separating domains whose discommensuration orientations differ by  $120^\circ$ . The kinks are themselves ordered and produce a structure in which two of the three possible rotationally equivalent domains of the  $(p \times \sqrt{3})$  reconstruction alternate across the surface. We call this the chevron phase. Recently, we have learned of scanning-tunneling-microscopy results which lead to the same structural model.<sup>13</sup> At 865 K, the reconstruction begins to lose long-range order. The first-order phase transformation to a disordered phase is complete by 880 K. In this phase, the recon-

struction exhibits hexagonal symmetry and the surface layer is isotropically compressed relative to the bulk (111) planes. Remarkably, the translational correlation length is only weakly temperature dependent (100 Å) between 900 and 1250 K. We call this the discommensuration-fluid phase.<sup>14</sup>

Measurements were performed on beam line X20A at the National Synchrotron Light Source. A (111)-oriented disk [mosaic  $0.02^\circ$  half width at half maximum (HWHM)], 10 mm in diameter and 2 mm thick, was studied by both glancing-incidence and x-ray reflectivity techniques. For the glancing-incidence measurements reported here, a radial resolution of  $0.0005 \text{ \AA}^{-1}$  HWHM and a transverse resolution of  $0.0001 \text{ \AA}^{-1}$  HWHM were achieved. The sample was supported within a chamber which itself mounts onto a standard diffractometer. At elevated temperatures the pressure in the chamber was typically  $3 \times 10^{-9}$  Torr. Our sample preparation procedures followed those given in Ref. 15. A complete account is presented in Ref. 16.

Figures 1(a)-1(d) illustrate the  $H$ - $K$  plane of reciprocal space for a reconstructed Au(111) surface. Open circles represent lateral periodicities of the bulk crystal (truncation rods). The solid symbols surrounding each truncation rod arise from the reconstruction (surface rods). We have used different symbols (solid circles, solid squares, and solid triangles) to distinguish scattering from the three domains. For convenience, we employ a hexagonal coordinate system  $(H, K, L)$  with  $L$  the surface normal index. (The unit for in-plane positions is  $a^* = 4\pi/\sqrt{3}a$ , where  $a$  is the nearest-neighbor distance. At 300 K,  $a = 2.885 \text{ \AA}$ .) The small hexagon drawn about the (0,1) truncation rod in Fig. 1(a) is reproduced in detail in Fig. 1(b), which shows the diffraction pattern expected for the  $(p \times \sqrt{3})$  reconstruction. In this figure, the surface rods are displaced from the truncation rod by  $\delta_D = 2\pi/L_D$ , where  $L_D = ap$  is the period of the discom-

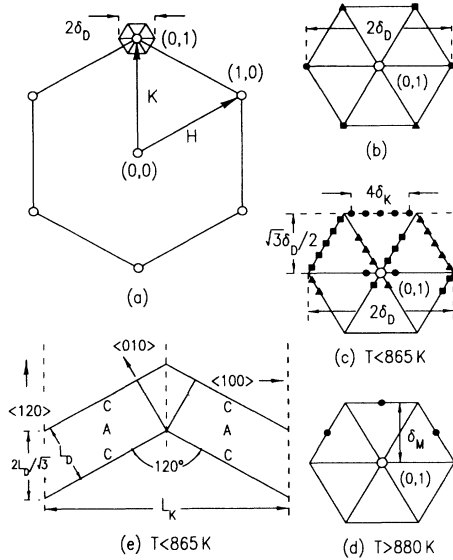


FIG. 1. (a)–(d) Diffraction pattern of a reconstructed Au(111) surface. Open circles are truncation rods, solid symbols are surface rods. (a) Reciprocal space as defined by the hexagonal coordinate system. The small hexagon about the (0,1) rod is reproduced in detail in (b)–(d). (b) (0,1) reflection of a uniaxially compressed surface.  $\delta_D$  is the discommensuration wave vector. Different symbols are used to indicate the scattering from three discommensuration domains. (c) (0,1) reflection observed in this study for  $T < 865$  K.  $\delta_K$  is the kink wave vector. (d) (0,1) reflection observed in this study for  $T > 880$  K.  $\delta_M$  is the misfit wave vector. (e) A chevron unit cell shown in hexagonal coordinates. The dotted lines are discommensurations. The solid line drawn in the  $\langle 010 \rangle$  direction corresponds to a  $(p \times \sqrt{3})$  reconstruction. Letters A and C indicate ABA-stacking and ABC-stacking regions, respectively.

mensuration structure. In contrast, the diffraction pattern obtained for  $T < 865$  K in our measurements is more complex. The hexagon about the (0,1) position is instead decorated with a multiplicity of peaks [Fig. 1(c)]. To index the observed peaks, it is necessary to introduce a second incommensurate wave vector ( $\delta_K$ ) in addition to  $\delta_D$ . At 300 K,  $\delta_K$  is close to  $0.2\delta_D$ .

The difference between the observed pattern [Fig. 1(c)] and that illustrated in Fig. 1(b) requires a more elaborate atomic arrangement than the  $(p \times \sqrt{3})$  reconstruction. It is clear, however, that the  $(p \times \sqrt{3})$  motif is an essential component of the Au(111) surface.<sup>1–10</sup> Therefore, it is natural to consider a structure composed of an ordered array of defects separating rotationally equivalent domains of the  $(p \times \sqrt{3})$  reconstruction. The simplest realization of this idea is a kink [Fig. 1(e)]. A periodic array of kinks separating two orientations of the  $(p \times \sqrt{3})$  motif produces a surface structure with a unit cell of dimensions  $L_K$  along the  $\langle 100 \rangle$  direction, where  $L_K$  is twice the separation between neighboring kinks, and  $2L_D/\sqrt{3}$  along the  $\langle 120 \rangle$  direction. The corresponding diffraction pattern consists of peaks separated by  $\delta_K$

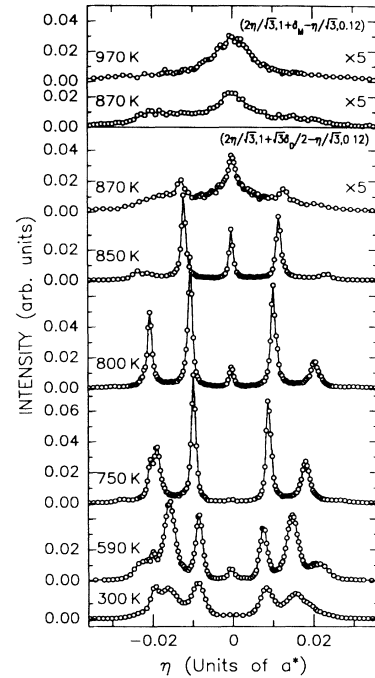


FIG. 2. Lower panel: transverse scans through  $(0,1 + \sqrt{3}\delta_D/2, 0.12)$  [see Fig. 1(c)]. Upper panel: transverse scans through  $(0,1 + \delta_M, 0.12)$  [see Fig. 1(d)]. Solid lines are guides to the eye. The two scans for 870 K were taken through different positions along the  $K$  direction.

( $= 2\pi/L_K$ ) and  $\sqrt{3}\delta_D/2$  in the  $\langle 2\bar{1}0 \rangle$  and the  $\langle 010 \rangle$  directions, respectively. The diffraction pattern [Fig. 1(c)] can be understood on this basis, provided that scattering from all three orientationally equivalent domains of the chevron reconstruction is included. No peaks appear at the hexagonal vertices, in contrast to the diffraction pattern for the  $(p \times \sqrt{3})$  structure.

We turn now to a description of the temperature dependence of the diffraction pattern by focusing on profiles transverse to the  $K$  direction, through  $K = 1 + \sqrt{3}\delta_D/2$ . This corresponds to the path shown as a dashed line along the top of the hexagon in Fig. 1(c). Results of scans at several temperatures are shown in Fig. 2. In the lower panel, each profile consists of a number of closely spaced peaks. With increasing temperature, the peak separation ( $\delta_K$ ) increases and a complicated evolution of the relative intensities and widths occurs. At 300 K, the peak at  $\eta = 0$  is very weak and the stronger peaks at  $\eta = \pm \delta_K$  and  $\eta = \pm 2\delta_K$  are relatively broad compared to equivalent peaks at higher temperatures. Also evident is that the widths of the peaks at  $\eta = \pm 2\delta_K$  are broader than those at  $\eta = \pm \delta_K$ . There are broad shoulders at  $\eta = \pm 3\delta_K$ , but they are too broad and weak to be clearly resolved at 300 K. The sharp features at  $\eta = \pm 0.02a^*$  occur at the vertices of the hexagon of Fig. 1(c), and correspond to the overlap of the current scan with the tails of the peaks that occur along

the other sides of the hexagon. At 590 K, the peaks at  $\eta=0$  and  $\eta = \pm 3\delta_K$  are more intense than at 300 K. In contrast, at 750 K, the peaks at  $\eta=0$  and  $\eta = \pm 3\delta_K$  are much weaker. Furthermore, the value of  $\delta_K$  has increased relative to its value at 590 K. At 800 K,  $\delta_K$  has increased still further and the peaks are noticeably narrower. The peak at  $\eta=0$  has considerable intensity again, while those at  $\pm 3\delta_K$  have disappeared. By 850 K, the peak at  $\eta=0$  has further intensified and those at  $\eta = \pm 2\delta_K$  have become weaker.

The temperature dependence of  $\delta_D$  and  $\delta_K$  is plotted in Fig. 3. Both wave vectors increase monotonically with increasing temperature; i.e., the chevron unit cell contracts relative to the bulk lattice. The discommensuration periodicity  $L_D$  varies smoothly from  $22.5a$  to  $300$  K to  $20.9a$  at  $850$  K, while the kink periodicity is approximately constant between  $300$  and  $700$  K ( $L_K=112.4a$ ), and decreases rapidly between  $700$  and  $850$  K (at  $850$  K,  $L_K=70.4a$ ). The ratio of the two wave vectors ( $\delta_K/\delta_D$ ) varies from  $\sim 0.2$  at  $300$  K to  $\sim 0.3$  at  $850$  K. Remarkably, the kink ordering extends farthest when the ratio is close to one-quarter. At one-quarter, the unit-cell dimensions are such that the distance along  $\langle 010 \rangle$  between kinks equals four discommensuration periods. It is important to add that calculated intensities based on the chevron structure quantitatively describe the observed variation of the peak intensities with the ratio  $\delta_K/\delta_D$ .<sup>16</sup> On this basis, the dramatic intensity changes evident in Fig. 2, which do not suggest *a priori* that a single structure is maintained between  $300$  and  $865$  K, may be simply accounted for.

The existence of an equilibrium density of kinks immediately suggests that competing interactions compromise to produce a structure characterized by the new wave vector ( $\delta_K$ ). Recently, it was proposed<sup>12</sup> that high-symmetry surfaces, which reconstruct into one of several, rotationally equivalent structures, are unstable to the formation of domains. This is because of the accompanying reduction of elastic stress induced in the

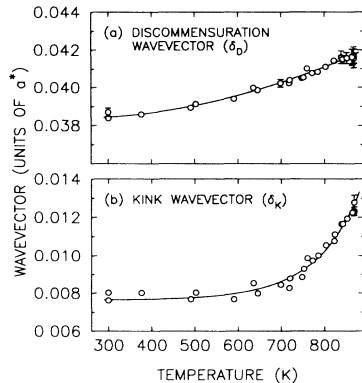


FIG. 3. Chevron reconstruction: Temperature dependence of (a) discommensuration wave vector  $\delta_D$  and (b) kink wave vector  $\delta_K$ . Solid lines are drawn to guide the eye.

bulk crystal. In the context of the Au(111) surface, the elastic energy is smaller for smaller kink separations, but this must be balanced against the energetic cost of disrupting the favorable ( $p \times \sqrt{3}$ ) structure at each kink. The competition between these two contributions determines  $\delta_K$ .<sup>17</sup> It is amusing to note that, since there are three rotationally equivalent domains of the chevron reconstruction, it may also be unstable to domain formation.

Above  $880$  K, we observe a partially disordered structure, which is characterized by the broad profiles shown in the upper panel of Fig. 2 and in Figs. 4(a) and 4(b). The observed diffraction pattern for this phase exhibits hexagonal symmetry [Fig. 1(d)]. The peak positions suggest that the surface layer is isotropically compressed with a periodicity  $L_M=4\pi/\sqrt{3}\delta_M$ . For  $T > 950$  K the scattering profile at  $(0,1+\delta_M)$  is well described by a Lorentzian in both the radial and transverse directions [solid lines in Figs. 4(a) and 4(b)]. The radial and transverse widths are plotted in Fig. 4(c) as a function of temperature. From the radial widths, we infer a correlation length of the order of  $\xi=35a$  ( $\sim 100$  Å). Analysis of the x-ray reflectivity<sup>16</sup> suggests that the ratio of regions with *ABA* stacking to regions with *ABC* stacking is preserved for all temperatures between  $300$  and  $1250$  K. We therefore call this structure a discommensuration fluid. Remarkably, the correlation length remains unchanged between  $950$  and  $1250$  K. As may be seen in Fig. 4(d), the misfit  $\delta_M$  increases with increasing tem-

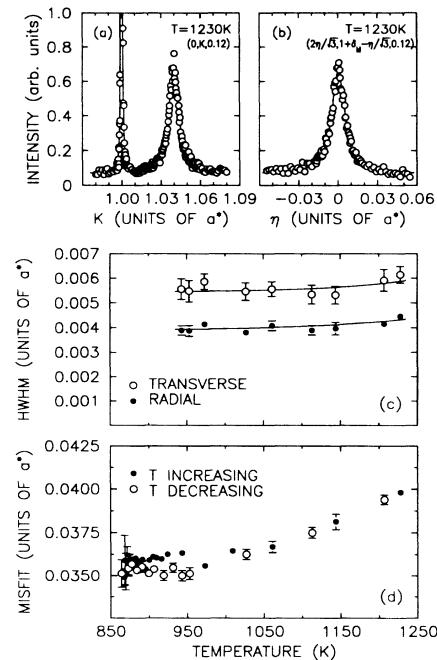


FIG. 4. Discommensuration-fluid phase: Typical (a) longitudinal and (b) transverse scans through a surface peak. Temperature dependence of (c) surface peak widths and (d) the misfit wave vector  $\delta_M$ .

perature: at 950 K,  $L_M = 28a$ ; at 1250 K,  $L_M = 25a$ . Evidently, the correlation length exceeds the surface periodicity by only a factor of  $\sim 1.4$ . In this respect, the discommensurations and kinks are very disordered.<sup>14</sup> Between 865 and 880 K, the surface scattering function is composed of two components with different radial positions—a narrow component corresponding to the chevron phase and a broad component corresponding to the discommensuration-fluid phase.<sup>16</sup> This coexistence is illustrated by the two transverse scans shown in Fig. 2 at 870 K, and indicates that the transformation between the two phases is first order.

The variation of the wave vectors with temperature in both phases implies that the overlayer contracts relative to the bulk lattice with increasing temperature. To gain additional insight we have calculated the area occupied by each surface atom. Specifically, we assume that the kinks do not change the surface density of the chevron phase, and that the density of the discommensuration-fluid phase is the same as if it were a hexagonal solid. Under these assumptions, the area per atom in the chevron phase decreases from  $0.826a^2$  at 300 K to  $0.824a^2$  at 865 K. Then there is a discontinuous increase in the areal density at the transformation from the chevron phase to the discommensuration-fluid phase. In the fluid phase, the area per atom continues to decrease with increasing temperature, from  $0.806a^2$  at 880 K to  $0.795a^2$  at 1250 K. The area per atom for a bulk (111) plane is  $0.866a^2$ , which is significantly larger. In contrast, the area per atom for the hexagonally reconstructed Au(001) surface is  $0.793a^2$  between 300 and 1170 K.<sup>15</sup> This is strikingly similar to the value for Au(111) at the highest temperatures, which suggests the possibility that a hexagonal overlayer of Au, on a Au substrate, has a natural lattice constant.<sup>11</sup>

In summary, we have studied the Au(111) surface structure between 300 and 1250 K, using x-ray diffraction. For  $T < 865$  K, the surface structure consists of an equilibrium density of kinks between rotationally equivalent domains of the  $(p \times \sqrt{3})$  reconstruction. The  $(p \times \sqrt{3})$  structure itself is composed of discommensurations separating ABC-stacking regions from ABA-stacking regions. Both the kink and discommensuration periodicities evolve to smaller values with increasing temperature. For  $T > 880$  K, we believe that atomic positions are well defined microscopically. However, the arrangement of kinks and discommensurations is disordered, giving rise to a structure which is isotropically

compressed. There is a first-order phase transformation between these two structures, involving a discontinuous change in the areal density.

We would like to thank D. D. Chambliss, B. M. Ocko, G. Ownby, and D. Vanderbilt. Work at BNL is supported by the DOE (DE-AC0276CH00016), at ORNL by the Division of Materials Sciences, DOE (DE-AC05-84OR21400) with Martin Marietta Energy Systems, Inc., and at MIT by the NSF (DMR-8806591). Beam line X20A is supported by the NSF (DMR-8719217) and by IBM.

<sup>1</sup>J. Perderau, J. P. Biberian, and G. E. Rhead, *J. Phys. F* **4**, 798 (1974).

<sup>2</sup>D. M. Zehner and J. F. Wendelken, in *Proceedings of the Seventh International Vacuum Congress and the Third International Conference on Solid Surfaces*, edited by R. Dobrozemsky *et al.* (Berger and Sohne, Vienna, 1977), p. 517.

<sup>3</sup>H. Melle and E. Menzel, *Z. Naturforsch.* **33a**, 282 (1978).

<sup>4</sup>J. C. Heyraud and J. J. Métois, *Surf. Sci.* **100**, 519 (1980).

<sup>5</sup>Y. Tanishiro, H. Kanamori, K. Takayanagi, K. Yagi, and G. Honjo, *Surf. Sci.* **111**, 395 (1981).

<sup>6</sup>L. D. Marks, V. Heine, and D. J. Smith, *Phys. Rev. Lett.* **52**, 626 (1984).

<sup>7</sup>U. Harten, A. M. Lahee, J. P. Toennies, and Ch. Wöll, *Phys. Rev. Lett.* **54**, 2619 (1985).

<sup>8</sup>W. J. Kaiser and R. C. Jaklevic, *Surf. Sci.* **182**, L227 (1987).

<sup>9</sup>Ch. Wöll, S. Chiang, R. J. Wilson, and P. H. Lippel, *Phys. Rev. B* **39**, 7988 (1989).

<sup>10</sup>M. M. Dovek, C. A. Lang, J. Nogami, and C. F. Quate, *Phys. Rev. B* **40**, 11973 (1989).

<sup>11</sup>R. J. Needs, and M. Mansfield, *J. Phys. Condens. Matter* **1**, 7555 (1989). See also, B. W. Dodson, *Phys. Rev. Lett.* **60**, 2288 (1988); R. J. Needs, *Phys. Rev. Lett.* **58**, 53 (1987).

<sup>12</sup>O. L. Alerhand, D. Vanderbilt, R. D. Meade, and J. D. Joannopoulos, *Phys. Rev. Lett.* **61**, 1973 (1988).

<sup>13</sup>D. D. Chambliss and R. J. Wilson (unpublished); J. V. Barth, H. Brune, G. Ertl, and R. J. Behm (unpublished).

<sup>14</sup>S. N. Coppersmith, D. S. Fisher, B. I. Halperin, P. A. Lee, and W. F. Brinkman, *Phys. Rev. B* **25**, 349 (1982); J. Villain and P. Bak, *J. Phys. (Paris)* **42**, 657 (1981).

<sup>15</sup>S. G. J. Mochrie, D. M. Zehner, B. M. Ocko, and D. Gibbs, *Phys. Rev. Lett.* **64**, 2925 (1990); D. Gibbs, B. M. Ocko, D. M. Zehner, and S. G. J. Mochrie, *Phys. Rev. B* **42**, 7330 (1990); B. M. Ocko, D. Gibbs, K. G. Huang, D. M. Zehner, and S. G. J. Mochrie (unpublished).

<sup>16</sup>A. R. Sandy, S. G. J. Mochrie, D. M. Zehner, K. G. Huang, and D. Gibbs (unpublished).

<sup>17</sup>D. Vanderbilt (unpublished).